IET Electric Power Applications

Research Article

ISSN 1751-8660
Received on 12th May 2019
Revised 20th July 2019
Accepted on 29th August 2019
doi: 10.1049/iet-epa.2019.0400
www.ietdl.org

Online maximum torque per ampere control for induction motor drives considering iron loss using input–output feedback linearisation

Hamidreza Mosaddegh Hesar[1], Hossein Abootorabi Zarchi[1] ✉, Mojtaba Ayaz Khoshhava[1]
[1]Department of Electrical Engineering, Faculty of Engineering, Ferdowsi University of Mashhad, Mashhad, Iran
✉ *E-mail: abootorabi@um.ac.ir*

Abstract: This study presents a novel online, accurate and simple model-based maximum torque per ampere (MTPA) strategy for input–output feedback linearisation control of induction motor (IM) drives. Despite conventional MTPA control principles which are under the assumption of iron loss neglecting, the proposed strategy takes iron loss effect into account. This study highlights the iron loss influence on MTPA scheme. Firstly, the cross-coupling effects in the IM model and torque non-linearity due to the iron loss in torque–speed characteristics of the IM are discussed. The criterion for the MTPA scheme is then introduced and investigated by gradient approach so that when the gradient vectors of the torque and stator current magnitude are parallel, the MTPA strategy is satisfied. Finally, to confirm the validity of the proposed control scheme, experiments are carried out.

Nomenclature

$\boldsymbol{V}, \boldsymbol{I}, \boldsymbol{\lambda}$	voltage, current, flux vectors
T_e	electromagnetic torque
T_l	load torque
R	resistance
R_i	iron loss resistance
L	self-inductance
L_l	leakage inductance
L_m	coupling inductance between stator and rotor
p	pole pair number of stator
ω_r	electrical rotor speed
ω	angular speed of rotor flux
ω_{slip}	slip speed
J	moment of inertia
σ	leakage factor $(1-(L_m^2/L_s \cdot L_r))$
α	angle between gradient vectors
δ	stator current angle
θ	rotor flux orientation angle

Subscripts

s, r	stator and rotor
d, q	rotating direct and quadrature axes

1 Introduction

Generally speaking, about 40% of the whole produced electrical energy in the world is consumed by electrical motors which are used in various applications such as pumps, fans, crushers, conveyors, mills, centrifugal machines, and elevators [1]. Various kinds of electrical motors have been designed for different applications. Among them, three-phase IMs possess the utmost part in industrial applications. Therefore, the optimal control of induction motor (IM) drives is appreciably important. The maximum torque per ampere (MTPA) strategies have shown to be very efficient methods for energy saving in IM drives. Indeed, the purpose of the MTPA algorithm is to produce a desired electrical torque with minimum stator current magnitude. Consequently, implementing MTPA strategy leads to minimum copper loss and since it possesses the great part of total losses, motor efficiency enhances [2]. Broadly speaking, there are two main approaches for MTPA realisation: search-based and model-based algorithms.

1.1 Search-based techniques

The principle of search-based approaches is to find the minimum stator current magnitude for a given speed and load torque. The main advantage of these methods is that the exact motor parameters and load condition information are not needed. Accordingly, they could be implemented for various kinds of motors with different control schemes [3]. In [4, 5], the vector control in combination with a search-based MTPA strategy is implemented for an IM drive. In the proposed MTPA method, the control parameter is the stator flux. However, the step change in the control parameter results in torque disturbances and consequently speed oscillations and even system instability. In [6], the conventional direct torque and flux control is performed and a maximum efficiency strategy has been realised determining the optimal flux level for a desired load torque and speed. In the proposed algorithm, for determining the minimum stator current magnitude, the stator flux is reduced stepwise from its nominal value and in each step, the stator current magnitude is measured. It should be noted that since the iron loss effect is not considered, the proposed control strategy is different from efficiency optimisation. In [7], the MTPA strategy is realised in the steady-state operation. In the proposed strategy, which is also based on a search algorithm, the saturation effect is taken into account. Owing to the slow nature of the search-based algorithms, the application of this method is also limited to narrow range torque variations. In the proposed strategy in [8], the optimal flux for the desired load torque is determined by the look-up table. This strategy is realised regardless of the iron loss which obviously deviates true MTPA realisation.

1.2 Model-based techniques

These methods which are based on the electrical model of motors are easy to implement and require the exact motor parameter values. Wasynczuk *et al.* [9] propose an MTPA strategy based on slip speed regulation which is implemented by indirect field-oriented control (FOC) in the rotor flux reference frame. To realise the strategy, the slip speed and the rotor time constant should be equal. As a result, the d–q-axis stator currents are equalised, which is the MTPA realisation criterion without taking the IM iron loss

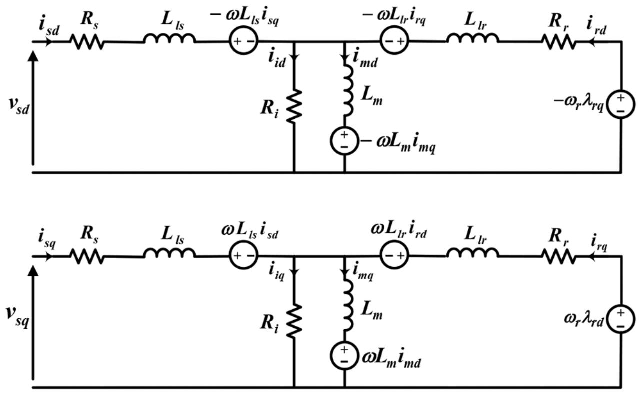

Fig. 1 *d–q-axis equivalent circuit of an IM in rotor flux frame considering iron loss*

into account. However, compared to the conventional FOC, the constant slip speed leads to slower torque dynamic response. The proposed FOC-based MTPA strategy in [10] calculates the online torque per ampere ratio and adds a correction term to the rotor flux angular position. It should be noted that, due to the variation of the transformation angle, the proposed strategy has slower dynamic response in comparison with the conventional FOC. Moreover, the variation of the correction term, which is a significant parameter for the dynamic response, may lead to torque fluctuations. In [11], the torque expression is introduced in terms of stator current magnitude and slip speed and the maximum torque is plotted versus stator current curve. Then, the stator current magnitude in terms of the maximum torque is derived through curve fitting. The slip speed as a function of the maximum torque is also derived. Consequently, for the desired load torque, the slip speed and the stator current magnitude, which lead to MTPA realisation, are determined. The proposed strategy neglects the iron loss effect on the MTPA realisation. In [12], the same authors have proposed another MTPA strategy, which takes the iron loss into account. In this reference, the effect of temperature variations on the reference stator current magnitude and slip speed, determined by the strategy proposed in [11], has been also studied. The results clarified that the temperature variations have a negligible effect on the reference stator current magnitude; however, it significantly varies the reference slip speed. In [13], a predictive MTPA strategy is proposed based on direct torque and flux control and without considering iron loss. The effectiveness of this strategy is limited to high torque and high speed applications.

Generally, the parameter-based MTPA strategies have much faster dynamic response in comparison with the search-based algorithms. Indeed, in the optimal flux search methods, if there exists a disturbance or a sudden change in the load torque, the flux command should be changed quickly. Otherwise, instability, due to inadequate flux and relatively slow convergence of the optimisation algorithm, is possible [14]. In most industrial applications such as electric vehicles, the motor operating point changes continuously and a control system with the high dynamic response is essential. Therefore, utilising search-based control strategies is not beneficial for these applications. On the other hand, the model-based MTPA algorithms, in addition to their quick dynamic response, can operate reliably in disturbance and for different load profiles. This study belongs to the model-based category.

In this study, the input–output feedback linearisation (IOFL) non-linear control in combination with an improved MTPA strategy for a three-phase IM drive is proposed taking into account the iron loss. According to this control approach, the error signals of the MTPA criterion and torque command with respect to the measured values are given to the non-linear controller derived considering the iron loss. The realisation criterion of the proposed MTPA strategy is obtained by Lagrange's theorem. In this regard, if the IM torque and stator current magnitude gradient vectors become parallel in the desired point, the MTPA will be realised. The iron loss, as a possible source of performance deterioration in the MTPA strategy, has hardly received any attention, so far. In the model-based approaches, to determine the MTPA factor, the iron loss resistance is usually disregarded in the torque equation due to the simplicity that this approximation will certainly deviate true loss minimisation implementation. On the contrary, in our proposed strategy, the optimal relation of *d*–*q*-axis stator currents is derived considering the iron loss and without any approximation. Obviously, the proposed strategy has a high accuracy in all operation conditions. Also, in this study, the iron loss effect on the behaviour of the drives is highlighted and to overcome the performance deterioration of IM drive arising from considering the iron loss, a rotor-flux estimator block is used by using the two-axis equations of IM [15]. The fundamental iron loss is identified through some effective experiments and the speed-dependent equivalent iron loss resistance required for the MTPA control is obtained from these data.

A detailed description of the proposed control strategy will be presented in the following sections. This paper is organised as follows: Section 2 describes the IM model including iron loss. In Section 3, the criterion for the MTPA scheme is introduced. The IOFL is developed for IM in Section 4. In Section 5, the experimental results are presented. Section 6 contains the concluding remarks.

2 IM model including iron loss

The orthogonal *d*–*q*-axis model of an IM including the iron loss is shown in Fig. 1. As illustrated, the iron loss is modelled by a resistance paralleled with the magnetising branch. A two-axis dynamic model of IM in the rotor-flux oriented reference frame is expressed as follows [15]:

$$v_{sd} = R_s i_{sd} + \mathrm{d}\lambda_{sd}/\mathrm{d}t - \omega\lambda_{sq} \quad (1)$$

$$v_{sq} = R_s i_{sq} + \mathrm{d}\lambda_{sq}/\mathrm{d}t + \omega\lambda_{sd} \quad (2)$$

$$v_{rd} = 0 = R_r i_{rd} + \mathrm{d}\lambda_{rd}/\mathrm{d}t - (\omega - \omega_r)\lambda_{rq} \quad (3)$$

$$v_{rq} = 0 = R_r i_{rq} + \mathrm{d}\lambda_{rq}/\mathrm{d}t + (\omega - \omega_r)\,\lambda_{rd} \quad (4)$$

$$\lambda_{sd} = L_{ls} i_{sd} + L_m i_{md} \quad \lambda_{sq} = L_{ls} i_{sq} + L_m i_{mq} \quad (5)$$

$$\lambda_{rd} = L_{lr} i_{rd} + L_m i_{md} \quad \lambda_{rq} = L_{lr} i_{rq} + L_m i_{mq} \quad (6)$$

$$\begin{aligned} R_i i_{id} &= L_m \mathrm{d}i_{md}/\mathrm{d}t - \omega L_m i_{mq} \\ R_i i_{iq} &= L_m \mathrm{d}i_{mq}/\mathrm{d}t + \omega L_m i_{md} \end{aligned} \quad (7)$$

$$T_e = \frac{3p}{2}(L_m/L_r)(\lambda_{rd}(i_{sq} - i_{iq}) - \lambda_{rq}(i_{sd} - i_{id})) \quad (8)$$

The rotor FOC is defined with the following constraints:

$$\lambda_{rd} = |\lambda_r| \quad \lambda_{rq} = 0 \quad (9)$$

By considering the constraints given by (9), the rotor voltage equations expressed in the rotor flux-oriented reference frame can

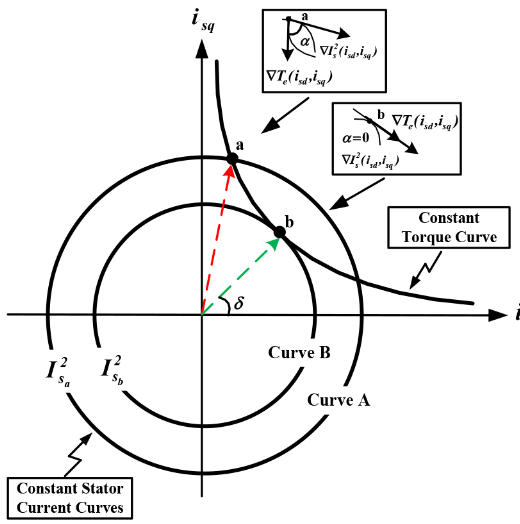

Fig. 2 *Constant torque curve and stator current curves*

be used to obtain the rotor magnetising current space vector ($\boldsymbol{i}_{\mathrm{m}}$) and slip speed ($\omega_{\mathrm{slip}}$).

Substitution of (6) into (3) and (4) yields the following rotor voltage differential equation:

$$0 = \frac{R_{\mathrm{r}}}{L_{\mathrm{lr}}}\boldsymbol{\lambda}_{\mathrm{r}} - \frac{R_{\mathrm{r}}L_{\mathrm{m}}}{L_{\mathrm{lr}}}\boldsymbol{i}_{\mathrm{m}} + \frac{\mathrm{d}\boldsymbol{\lambda}_{\mathrm{r}}}{\mathrm{d}t} + \mathrm{j}\omega_{\mathrm{slip}}\boldsymbol{\lambda}_{\mathrm{r}} \tag{10}$$

By decomposing into real- and imaginary-axis components, the following equations are obtained, which describe the flux model in the rotor flux-oriented reference frame

$$0 = \frac{R_{\mathrm{r}}}{L_{\mathrm{lr}}}|\boldsymbol{\lambda}_{\mathrm{r}}| - \frac{R_{\mathrm{r}}L_{\mathrm{m}}}{L_{\mathrm{lr}}}i_{\mathrm{m}d} + \frac{\mathrm{d}|\boldsymbol{\lambda}_{\mathrm{r}}|}{\mathrm{d}t} \Rightarrow L_{\mathrm{m}}i_{\mathrm{m}d} = |\boldsymbol{\lambda}_{\mathrm{r}}| + T_{\mathrm{r}}\frac{\mathrm{d}|\boldsymbol{\lambda}_{\mathrm{r}}|}{\mathrm{d}t} \tag{11}$$

$$0 = -\frac{R_{\mathrm{r}}L_{\mathrm{m}}}{L_{\mathrm{lr}}}i_{\mathrm{m}q} + \omega_{\mathrm{slip}}|\boldsymbol{\lambda}_{\mathrm{r}}| \Rightarrow \omega_{\mathrm{slip}} = \frac{L_{\mathrm{m}}}{T_{\mathrm{r}}|\boldsymbol{\lambda}_{\mathrm{r}}|}i_{\mathrm{m}q} \tag{12}$$

In the rotor FOC, by taking the iron loss into account, the output torque is conveniently described as

$$T_{\mathrm{e}} = \left(\frac{1}{\beta^2+1}\right)\cdot\left(\frac{R_{\mathrm{i}}}{\omega L_{\mathrm{lr}}}\right)\left(\beta i_{sq}\lambda_{\mathrm{r}d} - i_{sd}\lambda_{\mathrm{r}d} - \frac{\lambda_{\mathrm{r}d}^2}{L_{\mathrm{lr}}}\right) \tag{13}$$

where $\beta = (R_i/\omega L_{\mathrm{lr}}) + (R_{\mathrm{i}}/\omega L_{\mathrm{m}})$.

In the next section, in order to access the MTPA realisation criterion, the torque expression is manipulated to an appropriate form.

3 Proposed MTPA strategy

3.1 Basic concept

In principle, the purpose of MTPA strategies is to deliver the desired torque with the lowest stator current magnitude. In this way, the copper loss is minimised and hence the overall system efficiency is increased, at least as long as the copper loss is dominant [2]. In this study, one of the novel MTPA solutions based on Lagrange's theorem is introduced. Based on this theorem, any control strategy can be realised when the torque and its corresponding objective function (OF) are tangents at a point or in other words their gradient vectors are parallel. To apply the MTPA strategy for an IM, the minimisation of inverter current for a given load torque is defined as the OF.

3.2 MTPA control

The MTPA strategy is realised with minimisation of stator current magnitude under the constraint of constant torque. So, as previously mentioned, the torque equation of IM must be rewritten according to a specific form. To perform the proposed MTPA strategy, (13) must be modified so that this equation becomes a function of orthogonal stator current components. So, (13) can be changed as follows (for proof see Appendix 1)

$$T_{\mathrm{e}} = \left(\frac{\beta^2-1}{\beta^2+1}\right)\cdot\left(\frac{R_{\mathrm{i}}}{\beta\omega}\right)\left(i_{sq}i_{sd} - \frac{i_{sq}^2}{\beta}\right) \tag{14}$$

In MTPA, the minimisation of stator current magnitude is selected as the OF. The square stator current I_{s}^2 is defined as

$$I_{\mathrm{s}}^2 = i_{sd}^2 + i_{sq}^2 \tag{15}$$

In this section, the minimisation of (15) is selected as OF under a given load torque. According to Fig. 2, the torque equation for rotor FOC (by considering the iron loss) can be drawn on the $i_{sd} - i_{sq}$-plane. It can also be shown that on this plane the square stator current curve takes the form of a circle. Supposing the constant torque constraint, if the operating point is set at point 'a' in Fig. 2, the curve 'A' is considered to be constant stator current curve (I_{sa}^2). If an operating point is set at 'b', the curve 'B' is another constant stator current curve (I_{sb}^2). Using Lagrange's theorem, the stator current magnitude is minimum when the constant torque curve and the stator current curve are tangent at a point, or in other words, the MTPA is achieved when their gradient vectors are parallel at the tangency point (see 'b' in Fig. 2), so that

$$\| \nabla T_{\mathrm{e}}(i_{sd}, i_{sq}) \|\| \nabla I_{\mathrm{s}}^2(i_{sd}, i_{sq}) \| \sin\alpha = 0 \tag{16}$$

where α is the angle between $\nabla T_{\mathrm{e}}(i_{sd}, i_{sq})$ and $\nabla I_{\mathrm{s}}^2(i_{sd}, i_{sq})$. Therefore, the criterion of the MTPA strategy realisation is obtained as follows:

$$y_1 = \| \nabla T_{\mathrm{e}}(i_{sd}, i_{sq}) \|\| \nabla I_{\mathrm{s}}^2(i_{sd}, i_{sq}) \| \sin\alpha \tag{17}$$

It is obvious that the control strategy is realised when y_1 is kept at zero. The cross-product of gradient vectors is calculated from the following equation:

$$\nabla T_{\mathrm{e}}(i_{sd}, i_{sq}) \times \nabla I_{\mathrm{s}}^2(i_{sd}, i_{sq}) = \det\begin{bmatrix} i & j & k \\ \dfrac{\partial T_{\mathrm{e}}}{\partial i_{sd}} & \dfrac{\partial T_{\mathrm{e}}}{\partial i_{sq}} & 0 \\ \dfrac{\partial I_{\mathrm{s}}^2}{\partial i_{sd}} & \dfrac{\partial I_{\mathrm{s}}^2}{\partial i_{sq}} & 0 \end{bmatrix} \tag{18}$$

So the criterion of MTPA realisation is achieved as follows:

$$y_1 = \frac{\partial T_{\mathrm{e}}}{\partial i_{sd}} \times \frac{\partial I_{\mathrm{s}}^2}{\partial i_{sq}} - \frac{\partial T_{\mathrm{e}}}{\partial i_{sq}} \times \frac{\partial I_{\mathrm{s}}^2}{\partial i_{sd}} = 0 \Rightarrow y_1 = i_{sq}^2 + \frac{2}{\beta}i_{sq}i_{sd} - i_{sd}^2 = 0 \tag{19}$$

Neglecting the iron loss ($R_{\mathrm{i}} \to \infty$), the MTPA realisation criterion for ideal IM is achieved. In this condition, the criterion presented in (19) is simplified as

$$y_1 = i_{sq}^2 - i_{sd}^2 = 0 \Rightarrow i_{sq} = \pm i_{sd} \tag{20}$$

Although in ideal condition, the optimal current angle is constant ($\delta = \tan^{-1} i_{sq}/i_{sd} = \pm\pi/4$), but in the non-ideal condition, to overcome the iron loss effect the stator current angle diverges from the ideal condition. This angle is smaller than $\pi/4$ and dependent on β-value. By doing some calculations on (19), we have

$$i_{sq} = \pm i_{sd}\xi \Rightarrow \delta = \tan^{-1}(\xi) \tag{21}$$

where $\xi = \left((\sqrt{\beta^2+1} - 1)/\beta\right)$ is the MTPA factor.

Equation (21) indicates that for realisation of MTPA in the motoring mode, the $i_{sq} - \xi i_{sd} = 0$ must be always fulfilled. Hence,

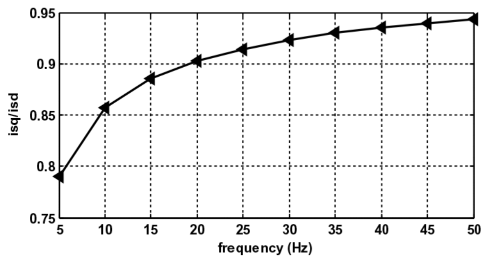

Fig. 3 *Variation of* $\xi = i_{sq}/i_{sd}$ *value versus operating frequency*

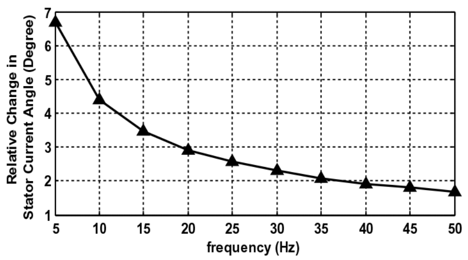

Fig. 4 *Relative change in stator current angle with frequency*

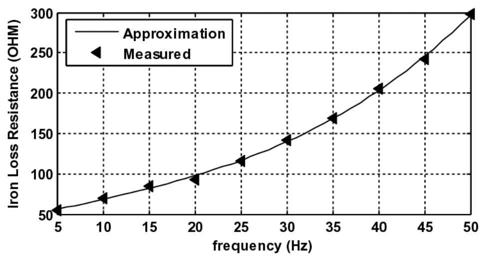

Fig. 5 *Identified values of equivalent iron loss resistance for the 2.2 kW IM*

it is necessary that the value of ξ is determined for each given speed (frequency). In Fig. 3, variation of ξ versus operating frequency has been plotted.

Fig. 4 shows the deviation of stator current angle from $\pi/4$ in various frequencies due to the iron loss.

3.3 Measurement of iron loss resistance

According to Fig. 5, experimentally identified equivalent iron loss resistance values of 2.2 kW IM can be acquired by measuring the input power at the no-load test. In this condition, the energetic balance of an IM can be expressed by the relation:

$$P_{\text{no-load}} = P_{\text{iron}} + P_{\text{cu,s}} + P_{\text{mech}} \tag{22}$$

where P_{iron} is the iron loss, $P_{\text{cu,s}}$ is the stator copper loss, and P_{mech} is the friction and windage loss. Along with [16], the previous expression allows to compute the iron loss, as the difference between the input power $P_{\text{no-load}}$ and the other losses items. A plot of iron loss versus rotor speed can be constructed for use in determining the iron loss at any desired rotor speed. Although R_{i} varies with the operating frequency and the flux level, it is more sensitive to variation of frequency rather than the rotor flux variations [17, 18].

4 IOFL for IM

In this section, the IOFL non-linear controller is applied to the IM drive system to obtain the control inputs for space vector modulation inverter. Therefore, by choosing $x_1 = i_{sd}$, $x_2 = i_{sq}$, $x_3 = \lambda_{rd}$, $x_4 = \lambda_{rq}$ and $x_5 = \omega_{\text{r}}$ as state variables and assuming $V_{sd}^* = u_1$, $V_{sq}^* = u_2$ as the control inputs, the IM affine model is described by

$$\dot{X} = f(X) + g(X)U \tag{23}$$

where

$$X = [x_1\ x_2\ x_3\ x_4\ x_5]^{\text{T}} = [i_{sd}\ i_{sq}\ \lambda_{sd}\ \lambda_{sq}\ \omega_{\text{r}}]^{\text{T}}, \tag{24}$$

$$U = [u_1\ u_2]^{\text{T}}, \tag{25}$$

(see (26)) and

$$g(X) = [g_1\ g_2] = \frac{1}{\sigma L_{\text{s}}} \cdot \frac{R_{\text{i}}}{R_{\text{i}} + R_{\text{s}}} \begin{bmatrix} 1 & 0 \\ 0 & 1 \\ 0 & 0 \\ 0 & 0 \\ 0 & 0 \end{bmatrix} \tag{27}$$

Choosing the magnitude of the cross product of $\nabla T_{\text{e}}(x_1, x_2)$ and $\nabla I_{\text{s}}^2(x_1, x_2)$ and the IM torque as controlled output, the output vectors can be introduced as

$$Y = \begin{bmatrix} y_1 \\ y_2 \end{bmatrix} = \begin{bmatrix} \| \nabla T_{\text{e}}(x_1, x_2) \| \| \nabla I_{\text{s}}^2(x_1, x_2) \| \sin\alpha \\ T_{\text{e}} \end{bmatrix} \tag{28}$$

Now, taking the time derivatives of outputs, we have

$$\begin{aligned} \begin{bmatrix} \dot{y}_1 \\ \dot{y}_2 \end{bmatrix} &= \begin{bmatrix} L_{\text{f}} y_1 \\ L_{\text{f}} y_2 \end{bmatrix} + \begin{bmatrix} L_{\text{g1}} y_1 & L_{\text{g2}} y_1 \\ L_{\text{g1}} y_2 & L_{\text{g2}} y_2 \end{bmatrix} \begin{bmatrix} u_1 \\ u_2 \end{bmatrix} \\ &= \begin{bmatrix} L_{\text{f}} y_1 \\ L_{\text{f}} y_2 \end{bmatrix} + E(X)U \end{aligned} \tag{29}$$

where $L_{\text{f}} y_i$, $i = 1, 2$ are the directional (or Lie) derivative of state function $y(x): R^n \to R$ along a vector field $f(x) = [f_1(x), \ldots, f_n(x)]$:

$$L_{\text{f}} y(x) = \sum_{i=1}^{n} \frac{\partial y(x)}{\partial x} f_i(x) \tag{30}$$

$$f(X) = [f_1\ f_2\ f_3\ f_4\ f_5]^{\text{T}}$$
$$= \begin{bmatrix} \dfrac{L_{\text{m}}}{\sigma L_{\text{s}} L_{\text{r}}} \left(\dfrac{1}{T_{\text{r}}} (x_3 - L_m \cdot x_1) + x_4 \cdot x_5 \right) - \dfrac{1}{\sigma L_{\text{s}}} (R_{\text{i}} \parallel R_{\text{s}}) \cdot x_1 + \omega \cdot x_2 \\ \dfrac{L_{\text{m}}}{\sigma L_{\text{s}} L_{\text{r}}} \left(\dfrac{1}{T_{\text{r}}} (x_4 - L_{\text{m}} \cdot x_2) - x_3 \cdot x_5 \right) - \dfrac{1}{\sigma L_{\text{s}}} (R_{\text{i}} \parallel R_{\text{s}}) \cdot x_2 - \omega \cdot x_1 \\ \dfrac{-1}{T_{\text{r}}} (x_3 - L_{\text{m}} \cdot x_1) + \omega \cdot (x_4 + L_{\text{lr}} \cdot x_2) - x_4 \cdot x_5 - \omega \cdot L_{\text{lr}} \cdot x_2 \\ \dfrac{-1}{T_{\text{r}}} (x_4 - L_{\text{m}} \cdot x_2) - \omega \cdot (x_3 + L_{\text{lr}} \cdot x_1) + x_3 \cdot x_5 + \omega \cdot L_{\text{lr}} \cdot x_1 \\ \dfrac{K_{\text{T}}}{J} \left(x_1 \cdot x_2 - \dfrac{x_2^2}{\beta} \right) - \dfrac{T_{\text{l}}}{J} \end{bmatrix}, \tag{26}$$

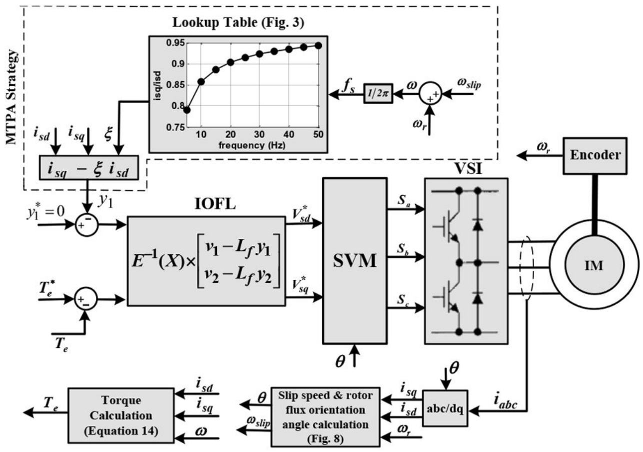

Fig. 6 *Proposed MTPA control strategy for rotor-FOC-based IM drives including iron loss*

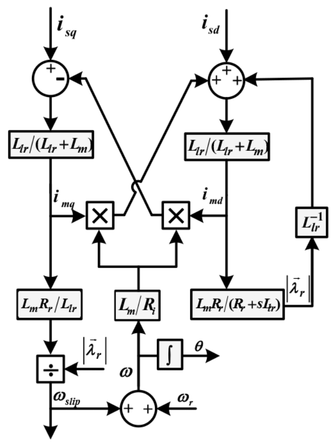

Fig. 7 *Slip speed and rotor flux orientation angle calculation considering iron loss*

$L_f y_i$ are given in Appendix 2. If the decoupling matrix $\boldsymbol{E}(X)$ is not singular, the non-linear control law is given by

$$\boldsymbol{U} = \begin{bmatrix} u_1 \\ u_2 \end{bmatrix} = \boldsymbol{E}^{-1}(X) \cdot \begin{bmatrix} v_1 - L_f y_1 \\ v_2 - L_f y_2 \end{bmatrix} \tag{31}$$

where v_1 and v_2 are the system new inputs. Assuming the following state variables as

$$\begin{aligned} \dot{y}_1 &= v_1 \\ \dot{y}_2 &= v_2 \end{aligned} \tag{32}$$

The system control efforts are chosen by

$$\begin{aligned} v_1 &= \dot{y}_{1,\mathrm{ref}} - K_1 e_1 \\ v_2 &= \dot{y}_{2,\mathrm{ref}} - K_2 e_2 \end{aligned} \tag{33}$$

where K_1 and K_2 are positive constants and $e_1 = y_1 - y_{1,\mathrm{ref}}$ and $e_2 = y_2 - y_{2,\mathrm{ref}}$. Therefore, the motor error dynamics are

$$\dot{e}_1 = -K_1 e_1, \quad \dot{e}_2 = -K_2 e_2 \tag{34}$$

Considering (34), for positive K_1 and K_2, e_1 and e_2 exponentially converge to zero. As seen, in the presented non-linear controller, two proportional–integral (PI) controllers employed in conventional IOFL are eliminated.

The overall block diagram of the proposed drive system is shown in Fig. 6. According to this configuration, the slip speed (ω_{slip}) calculation is necessary for MTPA strategy. Since the value of i_{mq} is not measurable, it is impossible to use (12). To solve this

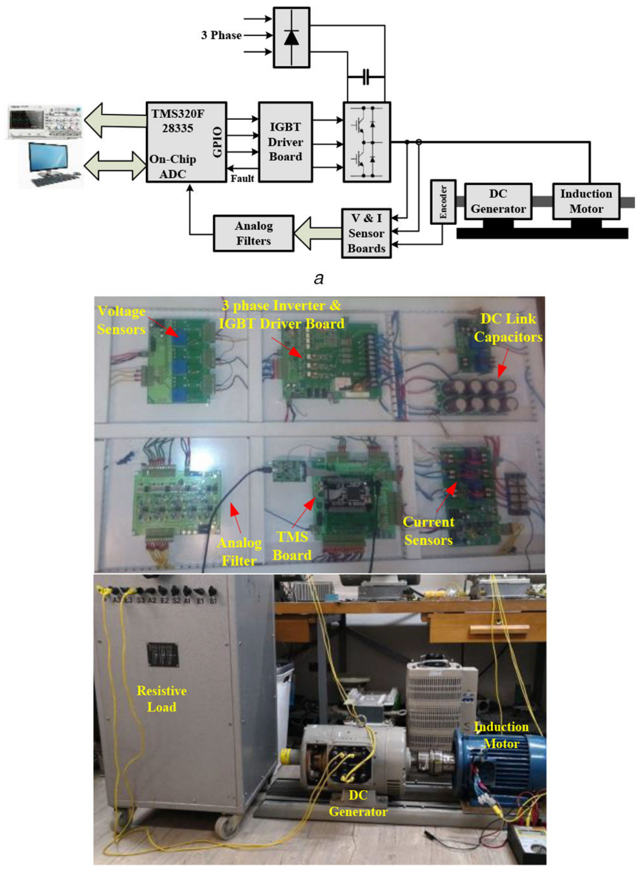

a

b

Fig. 8 *Experimental setup*
(a) Laboratory implementation block diagram, ***(b)*** IM drive system hardware

problem, a block diagram is derived considering (6) and (7) which is shown in Fig. 7. This scheme is applicable for flux rotor estimation with iron loss compensation. In this estimator, by measuring the stator current and rotor speed, the slip speed and rotor flux orientation angle (θ) are calculated.

5 Experimental setup and results

The performance of the proposed system is evaluated through a digital signal processor (DSP)-based prototype system. The experimental setup shown in Fig. 8 consists of a 2.2 kW IM, a voltage source inverter with a corresponding driver board, a sensor board and a TMS320F28335 signal processor board designed by Texas Instrument Co. The rotor speed is measured by a 1024 pulses incremental encoder mounted on the IM shaft. The stator phase currents are measured using two Hall-effect current sensors (LEM LTS-6-NP) and the line-to-line voltages are detected by voltage sensors (LEM LV-25-P). The experimental setup is also equipped with analogue second-order low-pass filters with 2.6 kHz cut-off frequency for filtering the measured stator current and voltage signals. The inverter is consist of insulated-gate bipolar transistor (IGBT) module SKM40GD124D (with 40 A, 1200 V ratings) and HCPL-316-J type intelligent IGBT drivers. These kinds of IGBT drivers provide electrical isolation between the power and the control systems. The switching frequency is selected 10 kHz for the inverter. In order to shoot through protection of inverter switches, the dead-time is 1 µs. It should be noted that the experimental setup is designed completely modular and the supply voltage for each of the boards is 24 versus DC. The calculated variables in the DSP are shown on the oscilloscope using the Digital to Analog Converter (DAC)-pulse-width modulation (PWM) output of DSP. Indeed the PWM value of the variable is converted to an analogue data through a low-pass filter. To measure the torque, a 3 kW separated excitation DC generator with an external rheostat in the armature terminal as a load is connected to

Table 1 IM parameters

Parameter	Value	Parameter	Value
pole-pair	2	R_r', Ω	0.6
rated torque, Nm	10	$L_{ls} = L_{lr}'$, H	0.00365
rated voltage, V	220 (L–L)	L_m, H	0.2933
R_s, Ω	0.76	—	—

Table 2 DC generator specifications

Parameter	Value	Parameter	Value
power, kW	4.8	rated current, A	21
rated voltage, V	230	rotor speed, rpm	1500

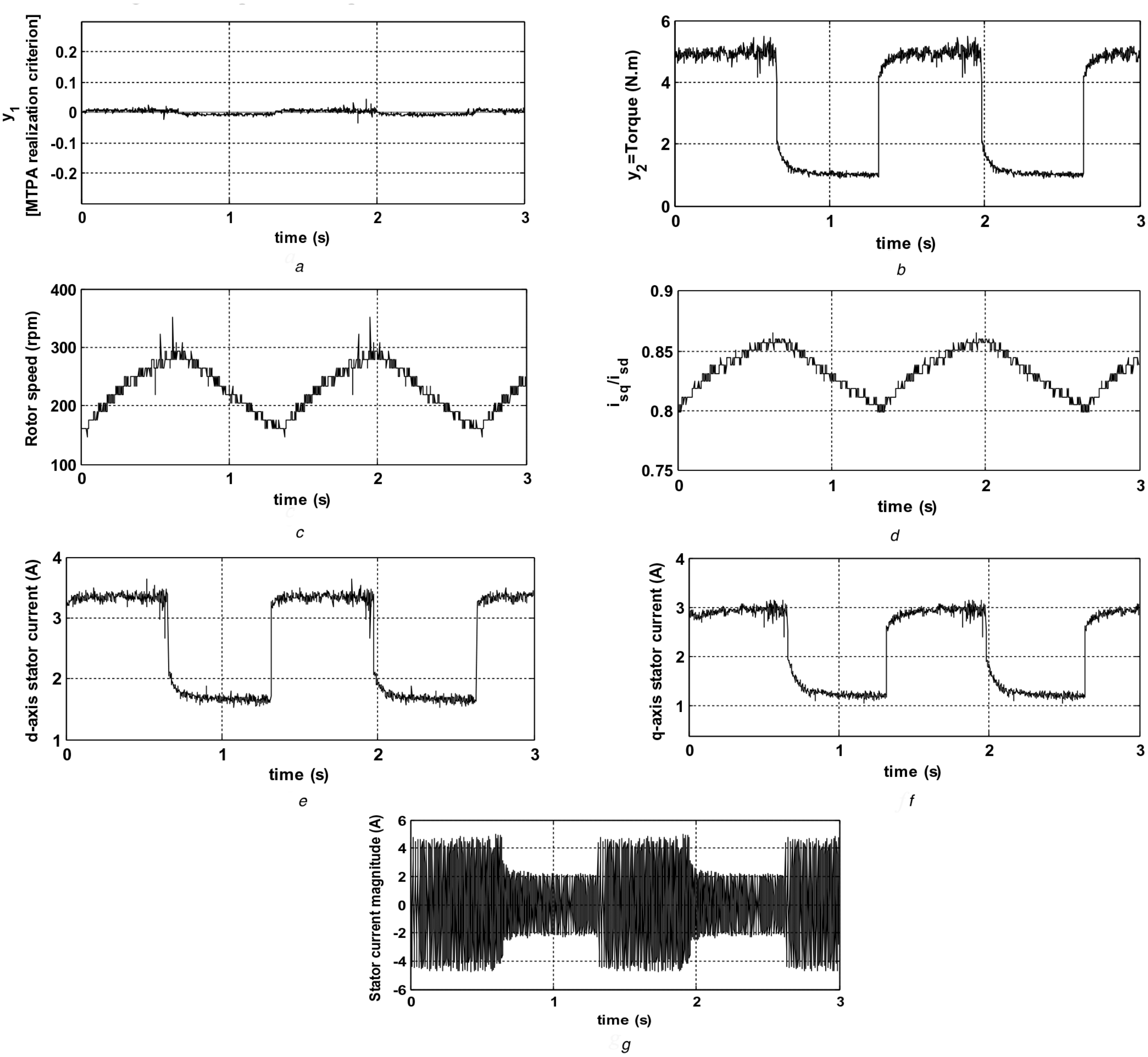

Fig. 9 *Experimental results of the proposed MTPA control*
(a) MTPA realisation criterion, ***(b)*** Electromagnetic torque, ***(c)*** Motor mechanical speed, ***(d)*** MTPA factor (ξ), ***(e)*** *d*-axis stator current, ***(f)*** *q*-axis stator current, ***(g)*** Stator current magnitude

the shaft of the IM. Tables 1 and 2 show the specifications and parameters of the 2.2 kW IM and DC generator, respectively.

Fig. 9*a* shows that the MTPA realisation criterion also tracks its reference value, which is zero, and the MTPA is, therefore, realised in both transient and steady-state conditions. As shown in Fig. 9*b* the electromagnetic torque tracks the step command torque properly. The rotor speed is illustrated in Fig. 9*c*. As depicted, the speed increases and decreases rather linearly as the desired torque is stepped up and stepped down. This clarifies that the non-linear controller is tuned appropriately. According to Fig. 3, the variation of the operating frequency changes the ξ parameter. In this regard, ξ is determined by the lookup table based on the speed variations

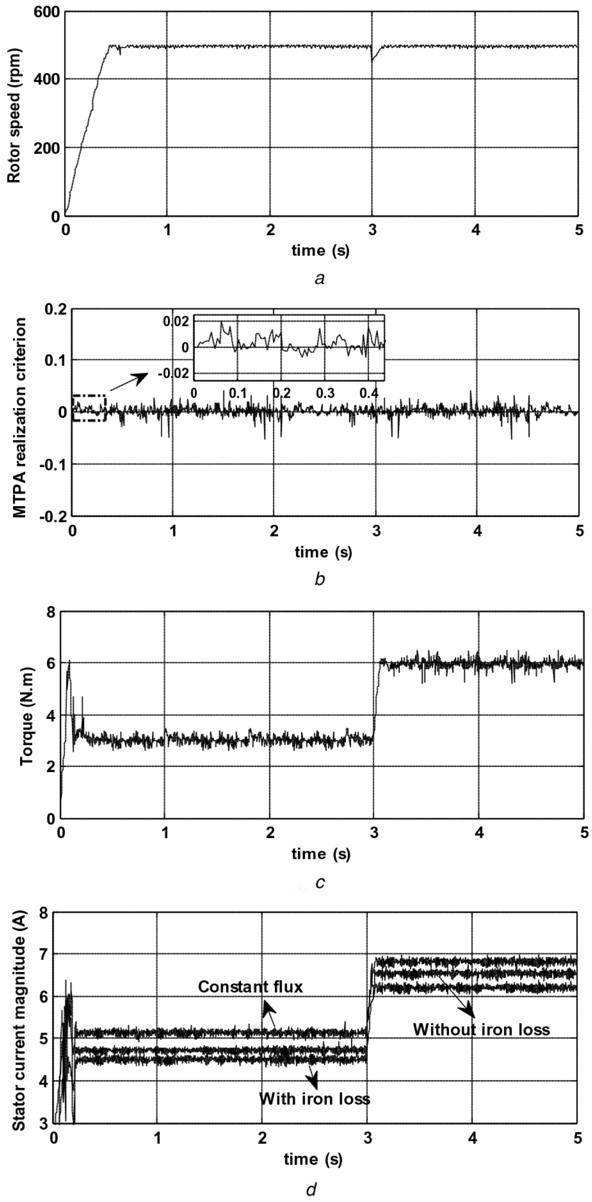

Fig. 10 *MTPA strategy operation with speed control*
(a) Motor mechanical speed, ***(b)*** MTPA realisation criterion, ***(c)*** Electromagnetic torque, ***(d)*** Stator current magnitude

(Fig. 9*d*). The *d*–*q*-axis stator currents are illustrated in Figs. 9*e* and *f*, respectively. Fig. 9*g* illustrates the stator phase current variations in response to the step torque command. To further study the proposed strategy, the performance of the MTPA strategy is investigated with closed-loop speed control. In this scheme, the speed error is delivered to the PI controller and torque command is then achieved from controller output. An exponential signal is applied for speed command and the experimental results are obtained for MTPA strategy, as shown in Fig. 10. In this condition, the load torque is stepped up from 3 to 6 Nm, at $t = 3\,\text{s}$. As illustrated, the rotor speed and electromagnetic torque properly follow their commands. Additionally, y_1 oscillates about its reference signal ($y_1^* = 0$). This guarantees that the MTPA strategy is realised. The stator current magnitude for this load torque step change is shown in Fig. 10*d*. In this figure, three scenarios are considered: constant flux, proposed MTPA (considering iron loss effect) and conventional MTPA (neglecting iron loss effect). To achieve the conventional FOC, the flux control loop is substituted with the control loop of MTPA strategy. Therefore, the flux command is set on the nominal value and the both speed and flux control are fulfilled. As is clear, implementing the proposed MTPA, the stator current magnitude decreases by about 7% in comparison with the conventional MTPA strategy.

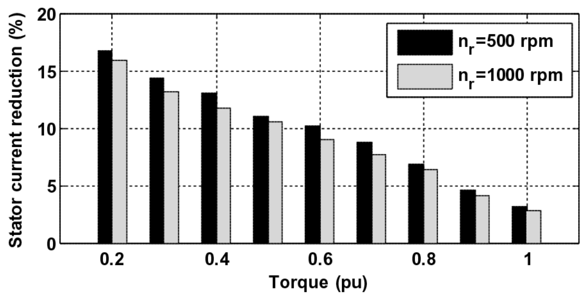

Fig. 11 *Stator current reduction with load torque changes*

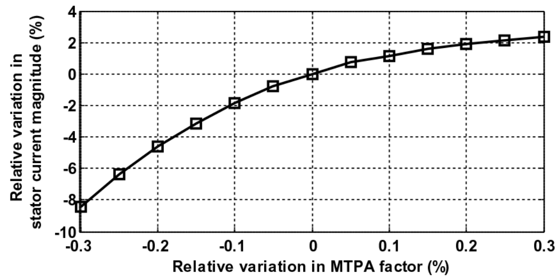

Fig. 12 *Relative change in stator current magnitude against error in ξ*

An additional scenario is carried out to further evaluate the performance of the proposed control scheme. In this regard, the proposed MTPA control is compared with the conventional FOC with rated flux. To investigate the overall operation of the proposed MTPA control at different rotor speeds and torques, the IM drive is controlled for $n_\text{r} = 500$ and 1000 rpm at various torques from light to nominal load (Fig. 11). The results show the superiority of the improved MTPA over the conventional FOC due to the possibility of adjusting the flux level for different load torques. As expected, the reduction of stator current magnitude is more significant at the light load conditions.

Model-based MTPA algorithms are expected to drift from the optimum with parameter variation. It is obvious that the MTPA criterion is dependent on the ξ value. The question then arises as to how accurately this parameter must be determined. To determine this, a sensitivity analysis is carried out to find the effect of inaccurate knowledge of ξ on the performance of this strategy. The result is plotted in Fig. 12. The conclusion which can be drawn from this plot is that MTPA is relatively insensitive to an error in ξ when it is in the range of −10% to +20%.

6 Conclusion

In this study, a non-linear controller based on the IOFL technique was merged with the online model-based MTPA control for a three-phase IM drives including the iron loss. The mechanism of iron loss influence on MTPA criterion was introduced and analysed based on Lagrange's theorem. As a result, it was found out the amount of detuning which is present when the iron loss is neglected in the execution of MTPA, depends on the machine operating frequency as well as its corresponding equivalent iron loss resistance. The validity of the improved MTPA controller was evaluated by experimental results. The experiments showed that by controlling the inverter current-minimising criterion directly, the MTPA scheme is executed online without deteriorating the dynamics performance. In addition, to demonstrate any benefits provided by the mentioned control scheme, the proposed MTPA strategy was compared with the conventional MTPA and the FOC with rated flux. It was shown by applying the improved MTPA control, the stator current magnitude was significantly less than the FOC with rated flux, especially at the light loads.

7 Acknowledgment

The authors wish to express appreciation to Research Deputy of Ferdowsi University of Mashhad for supporting this project by grant no. 48612 (9 January 2019).

8 References

[1] de Almeida, A.T., Ferreira, F.J.T.E., Baoming, G.: 'Beyond induction motors —technology trends to move-up efficiency', *IEEE Trans. Ind. Appl.*, 2014, **50**, (3), pp. 2103–2114

[2] Bolognani, S., Peretti, L., Zigliotto, M.: 'Online MTPA control strategy for DTC synchronous reluctance motor drives', *IEEE Trans. Power Electron.*, 2011, **26**, (1), pp. 20–28

[3] Abootorabi Zarchi, H., Mosaddegh Hesar, H., Ayaz Khoshhava, M.: 'Online maximum torque per power losses strategy for indirect rotor flux oriented control based induction motor drives', *IET Electr. Power Appl.*, 2019, **13**, (2), pp. 259–265

[4] Arab-Markadeh, G.R., Hajian, M., Soltani, J., *et al.*: 'Maximum torque per ampere control of sensor-less induction motor drives with DC offset and parameter compensation', *Energy Convers. Manage.*, 2010, **51**, (7), pp. 1354–1362

[5] Soltani, J., Hajian, M., Arab-Markadeh, G.R.: 'Maximum torque per ampere control of induction motor drive without mechanical sensor'. Int. Conf. on Control, Automation and Systems (ICCAS), Seoul, Republic of Korea, October 2008

[6] Kaboli, S., Zolghadri, M.R., Vahdati-Khajeh, E.: 'A fast flux search controller for DTC-based induction motor drives', *IEEE Trans. Ind. Electron.*, 2007, **54**, (5), pp. 2407–2416

[7] Bozhko, S., Dymko, S., Kovbasa, S., *et al.*: 'Maximum torque-per-amp control for traction IM drives: theory and experimental results', *IEEE Trans. Ind. Appl.*, 2017, **53**, (1), pp. 181–193

[8] Bojoi, R., Li, Z., Odhano, S.A., *et al.*: 'Unified direct-flux vector control of induction motor drives with maximum torque per ampere operation'. Energy Conversion Congress and Exposition (ECCE), Denver, CO, USA, September 2013

[9] Wasynczuk, O., Sudhoff, S.D., Corzine, K.A., *et al.*: 'A maximum torque per ampere control strategy for induction motor drives', *IEEE Trans. Energy Convers.*, 1998, **13**, (2), pp. 163–169

[10] Consoli, A., Scarcella, G., Scelba, G., *et al.*: 'Induction motor sensorless control based on a maximum torque per ampere approach'. 38th Industry Applications Conf. (IAS), Salt Lake City, UT, USA, October 2003

[11] Kwon, C., Sudhoff, S.D.: 'An adaptive maximum torque per amp control strategy'. IEEE Int. Conf. on Electric Machines and Drives, San Antonio, TX, USA, May 2005

[12] Kwon, C., Sudhoff, S.D.: 'An improved maximum torque per amp control strategy for induction machine drives'. 20th Applied Power Electronics Conf. (APEC), Austin, TX, USA, June 2005

[13] Ahmed, A., Kwon Koh, B., Kim, J., *et al.*: 'Finite control set-model predictive speed control for induction motors with optimal duration'. 20th IFAC World Congress, Toulouse, France, July 2017, vol. 50, no. 1, pp. 7801–7806

[14] Daryabeigi, E., Abootorabi Zarchi, H., Arab-Markadeh, G.R., *et al.*: 'Online MTPA control approach for synchronous reluctance motor drives based on emotional controller', *IEEE Trans. Power Electron.*, 2015, **30**, (4), pp. 2157–2166

[15] Levi, E., Sokola, M., Boglietti, A., *et al.*: 'Iron loss in rotor-flux-oriented induction machines: identification, assessment of detuning, and compensation', *IEEE Trans. Power Electron.*, 1996, **11**, (5), pp. 698–709

[16] Test procedure for poly-phase induction motors and generators, IEEE Standard 112 (Revision of IEEE Std 112-2004), 2017

[17] Levi, E.: 'Impact of iron loss on behavior of vector controlled induction machines', *IEEE Trans. Ind. Appl.*, 1995, **31**, (6), pp. 1287–1296

[18] Matsuse, K., Yoshizumi, T., Katsuta, S., *et al.*: 'High-response flux control of direct-field-oriented induction motor with high efficiency taking core loss into account', *IEEE Trans. Ind. Appl.*, 1999, **35**, (1), pp. 62–69

9 Appendix

9.1 Appendix 1

In this section, the detailed procedures for deriving the torque equation including the iron loss are presented. In the rotor FOC, the torque equation is given by (13). From (7) and writing $i_{\mathrm{m}d}$ in terms of $i_{\mathrm{i}q}$, we have

$$i_{\mathrm{m}d} = \frac{R_{\mathrm{i}} i_{\mathrm{i}q}}{\omega L_{\mathrm{m}}} \tag{35}$$

Substituting (35) into (6) gives (36)

$$\lambda_{\mathrm{r}d} = L_{\mathrm{lr}} i_{\mathrm{r}d} + L_{\mathrm{m}} \left(\frac{R_{\mathrm{i}}}{\omega L_{\mathrm{m}}} i_{\mathrm{i}q} \right) \tag{36}$$

Considering $i_{\mathrm{r}d} = i_{\mathrm{m}d} + i_{\mathrm{i}d} - i_{\mathrm{s}d}$, (36) is rewritten as:

$$\begin{gathered} i_{\mathrm{r}d} = \frac{R_{\mathrm{i}}}{\omega L_{\mathrm{m}}} i_{\mathrm{i}q} + \left(\frac{1}{1+\beta^2} \right) \left(i_{\mathrm{s}d} + \frac{\lambda_{\mathrm{r}d}}{L_{\mathrm{lr}}} - \beta i_{\mathrm{s}q} \right) - i_{\mathrm{s}d} \\ \Downarrow \\ \lambda_{\mathrm{r}d} = \frac{R_{\mathrm{i}}}{\omega} \left(1 + \frac{L_{\mathrm{lr}}}{L_{\mathrm{m}}} \right) i_{\mathrm{i}q} + L_{\mathrm{lr}} \left(\frac{1}{1+\beta^2} - 1 \right) i_{\mathrm{s}d} - \frac{\beta L_{\mathrm{lr}}}{1+\beta^2} i_{\mathrm{s}q} + \frac{\lambda_{\mathrm{r}d}}{1+\beta^2} \end{gathered} \tag{37}$$

Considering $i_{\mathrm{i}q} = i_{\mathrm{s}q} + \beta i_{\mathrm{s}d} + \beta \lambda_{\mathrm{r}d} / L_{\mathrm{lr}}$ and after a few manipulations, (13) is developed as

$$T_{\mathrm{e}} = \left(\frac{\beta^2 - 1}{\beta^2 + 1} \right) \cdot \left(\frac{R_{\mathrm{i}}}{\beta \omega} \right) \left(i_{\mathrm{s}q} i_{\mathrm{s}d} - \frac{i_{\mathrm{s}q}^2}{\beta} \right) \tag{38}$$

9.2 Appendix 2

$$L_f y_1 = f_2(x) - \xi \cdot f_1(x) \tag{39}$$

$$L_{\mathrm{f}} y_2 = K_{\mathrm{T}} \cdot \left(x_2 \cdot f_1(x) + \left(x_1 - \frac{2x_2}{\beta} \right) \cdot f_2(x) \right) \tag{40}$$

$$L_{g_1} y_1 = \frac{-\xi \cdot R_{\mathrm{i}}}{(\sigma \cdot L_{\mathrm{s}}) \cdot (R_{\mathrm{s}} + R_{\mathrm{i}})} \tag{41}$$

$$L_{g_2} y_1 = \frac{R_{\mathrm{i}}}{(\sigma \cdot L_{\mathrm{s}}) \cdot (R_{\mathrm{s}} + R_{\mathrm{i}})} \tag{42}$$

$$L_{g_1} y_2 = K_{\mathrm{T}} \cdot \left(\frac{R_{\mathrm{i}} \cdot x_2}{(\sigma \cdot L_{\mathrm{s}}) \cdot (R_{\mathrm{s}} + R_{\mathrm{i}})} \right) \tag{43}$$

$$L_{g_2} y_2 = K_{\mathrm{T}} \cdot \left(x_1 - \frac{2x_2}{\beta} \right) \cdot \left(\frac{R_{\mathrm{i}}}{(\sigma \cdot L_{\mathrm{s}}) \cdot (R_{\mathrm{s}} + R_{\mathrm{i}})} \right) \tag{44}$$

where $K_{\mathrm{T}} = \left((\beta^2 - 1)/(\beta^2 + 1) \right) \cdot (R_{\mathrm{i}} / \beta \omega)$.

The decoupling matrix $\boldsymbol{E}(X)$ is found to be non-singular for all operating regions except for null states by its determinant expressed in

$$\begin{aligned} \boldsymbol{E}(X) &= \begin{bmatrix} L_{g_1} y_1 & L_{g_2} y_1 \\ L_{g_1} y_2 & L_{g_2} y_2 \end{bmatrix} \\ &= \frac{R_{\mathrm{i}}}{(\sigma \cdot L_{\mathrm{s}}) \cdot (R_{\mathrm{s}} + R_{\mathrm{i}})} \begin{bmatrix} -\zeta & 1 \\ K_{\mathrm{T}} x_2 & K_{\mathrm{T}} \cdot \left(x_1 - \frac{2x_2}{\beta} \right) \end{bmatrix} \\ \det\,(\boldsymbol{E}(X)) &= \frac{R_{\mathrm{i}} \cdot K_{\mathrm{T}}}{(\sigma \cdot L_{\mathrm{s}}) \cdot (R_{\mathrm{s}} + R_{\mathrm{i}})} \left(\zeta \cdot \left(x_1 - \frac{2x_2}{\beta} \right) + x_2 \right) \end{aligned} \tag{45}$$